Crystal melting and black holes

hep-th/0610005
HUTP-06/A0039

Crystal Melting and Black Holes

Jonathan J. Heckman[1,*] and Cumrun Vafa[1,2†]

[1]Jefferson Physical Laboratory, Harvard University, Cambridge, MA 02138, USA

[2]Center for Theoretical Physics, MIT, Cambridge, MA 02139, USA

Abstract

It has recently been shown that the statistical mechanics of crystal melting maps to A-model topological string amplitudes on non-compact Calabi-Yau spaces. In this note we establish a one to one correspondence between two and three dimensional crystal melting configurations and certain BPS black holes given by branes wrapping collapsed cycles on the orbifolds $\mathbb{C}^2/\mathbb{Z}_n$ and $\mathbb{C}^3/\mathbb{Z}_n \times \mathbb{Z}_n$ in the large n limit. The ranks of gauge groups in the associated gauged quiver quantum mechanics determine the profiles of crystal melting configurations and the process of melting maps to flop transitions which leave the background Calabi-Yau invariant. We explain the connection between these two realizations of crystal melting and speculate on the underlying physical meaning.

October, 2006

*e-mail: jheckman@fas.harvard.edu
†e-mail: vafa@string.harvard.edu

1 Introduction

An important feature of string theory is how geometric data in a string compactification appear in the associated low energy effective theory. A striking example is provided by space-time filling brane probes of orbifold singularities. From the perspective of the quiver gauge theory, a topology-changing flop transition appears as a Seiberg-like duality which alters the ranks, matter content, and interaction terms of the gauge theory [1, 2]. It is therefore of interest to study the effect of flop transitions on more general brane configurations.

A related issue concerns what degrees of freedom in string theory replace macroscopic notions of classical geometry at small distance scales. In [3] it was shown that the target space formulation of the topological A-model on $\mathbb{C}^3$ describes quantum foam on the same geometry. Remarkably, the partition sum of this model is identical to that of three dimensional crystal melting [4]. In two dimensions, crystal melting adds squares to a 2d Young tableau. In three dimensions, crystal melting stacks cubes at the corner of a room. It is believed that other crystal melting models determine A-model amplitudes on more general non-compact Calabi-Yau spaces.

Topological strings have also recently appeared in the physics of four dimensional black holes. The work of [5] presented evidence that the indexed partition function for a mixed ensemble of four dimensional Calabi-Yau black holes with fixed magnetic charges and electric chemical potentials is determined by topological string theory on the same Calabi-Yau space. This suggests that other ensembles of black holes are also of relevance.

In this note we combine these themes and show that the crystal melting configurations of topological string theory are in one to one correspondence with certain BPS black holes given by branes wrapped on collapsed cycles in the supersymmetric orbifolds $\mathbb{C}^2/\mathbb{Z}_n$ and $\mathbb{C}^3/\mathbb{Z}_n \times \mathbb{Z}_n$ in the limit of large n. The black holes in this spectrum are generated by all possible flop transitions which leave the background Calabi-Yau geometry invariant, and the stability of these configurations is determined by the rigid structure of the partially melted crystal. Additionally, in both cases the duality group generated by these transitions corresponds to the Weyl group of an infinite dimensional algebra. The character of the basic representation of each algebra coincides with the corresponding partition sum over black hole charges. We believe that this technique of generating BPS spectra on a Calabi-Yau space using geometry preserving flop transitions may also be of use in a wider context than that

presented here.

At low energies, these charge configurations are well-described by gauged quiver quantum mechanics. The ranks of the gauge group factors determine D0- and D2-branes wrapped on collapsed cycles in $\mathbb{C}^2/\mathbb{Z}_n$ and D0-, D2- and D4-branes wrapped on collapsed cycles in $\mathbb{C}^3/\mathbb{Z}_n \times \mathbb{Z}_n$. In the limit of large charges, a stable configuration in $\mathbb{C}^2/\mathbb{Z}_n$ and $\mathbb{C}^3/\mathbb{Z}_n \times \mathbb{Z}_n$ will produce a local model for a BPS black hole in six and four dimensions, respectively. From the perspective of the effective theory, a flop transition which leaves the classical geometry invariant may alter the ranks of the gauge groups but will always preserve both the adjacency of bifundamentals in the quiver as well as the form of the superpotential.

In order to describe the precise action of flop transitions on $\mathbb{C}^3/\mathbb{Z}_n \times \mathbb{Z}_n$, we will find it necessary to treat the fractional branes of the orbifold theory as objects in the bounded derived category of coherent sheaves. Each basis of fractional branes is generated by a series of mutations on an exceptional collection of sheaves supported on a complex surface of the resolved geometry. Further, the exceptional collections appropriate for describing three dimensional crystal melting are all supported on a complex surface in the canonical smooth resolution of $\mathbb{C}^3/\mathbb{Z}_n \times \mathbb{Z}_n$.

Exceptional collections are most commonly used in the study of type IIB space-time filling D3-brane probes of local Calabi-Yau singularities [1, 2, 6, 7, 8]. We note that there are typically many exceptional collections which generate the *same* four dimensional quiver gauge theory. This suggests the presence of a large gauge symmetry or redundancy in the description of four dimensional quiver gauge theories in terms of exceptional sheaves. Indeed, in the case of four dimensional gauge theories, gauge anomaly considerations require that the rank assignments remain unchanged under flop transitions which preserve the classical geometry. A perhaps surprising result of this note is that in the more general case of BPS black holes described by gauged quiver quantum mechanics, different exceptional collections *will* produce different rank assignments in the quiver theory and will therefore break the gauge symmetry described above.

In our setup, the profile or "height" of the partially melted crystal is encoded in the ranks of gauge groups in the quiver theory. In some sense, this is to be expected. The target space formulation of topological string theory in terms of crystal melting in two and three dimensions corresponds to counting D0-brane bound states in the topologically twisted $U(1)$ gauge theories of a D4-brane and D6-brane filling $\mathbb{C}^2$ and $\mathbb{C}^3$, respectively. Since a D0-brane in the orbifolds $\mathbb{C}^2/\mathbb{Z}_n$ and $\mathbb{C}^3/\mathbb{Z}_n \times \mathbb{Z}_n$ lifts to n

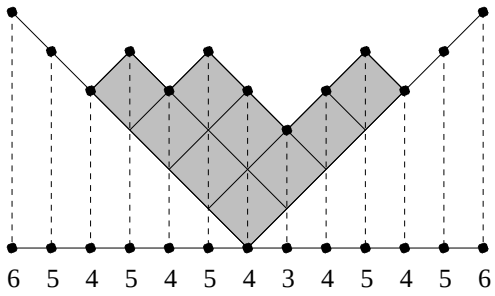

Figure 1: A 2d Young tableau defines a height function on the one dimensional lattice given by the integers. The numbers shown indicate height assignments for the given tableau. These heights are the rank assignments in the large n $\mathbb{C}^2/\mathbb{Z}_n$ quiver theory.

and n^2 image branes in $\mathbb{C}^2$ and $\mathbb{C}^3$ respectively, the untwisted RR D0-brane charge of the orbifold theory is up to a factor of $1/n$ and $1/n^2$ this sum in ranks. We now describe in more detail these crystal melting configurations.

As mentioned, the "height function" of the crystal specifies the ranks in the quiver theory. For 2d crystals, this integer valued function satisfies:

$$h(i) - h(i+1) = \pm 1 \tag{1}$$

for all integers i. The profile of this function is given by rotating the Young tableau by 135°. See figure (1) for an example. To describe heights for 3d crystals, we use dimer models. Recent reviews on the mathematical physics of dimer models are given in [9, 10].

A dimer model corresponds to a collection of black and white atoms on a bipartite lattice[1]. The atoms of the lattice correspond to vertices, the oriented links between black and white atoms are edges, and polygons constructed from the edges are faces of the dimer model. A perfect matching PM is defined as a collection of edges such that each vertex touches a single edge of PM.

For dimers on the plane, every perfect matching PM defines a unique integer valued height function h_{PM} up to the addition of a constant. Given two faces A and

[1]This is a lattice which admits a coloring of its vertices by black and white atoms so that no white atom connects to a black atom and vice versa.

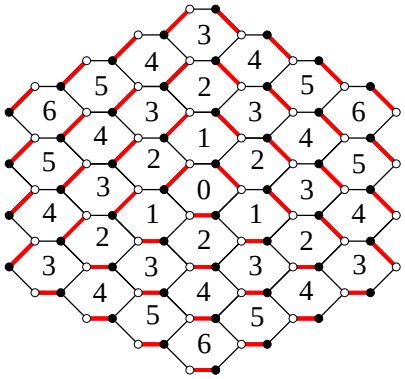

Figure 2: The empty room perfect matching (red). The integers at the center of each face indicate the value of the height function. These heights map to rank assignments in the $\mathbb{C}^3/\mathbb{Z}_n \times \mathbb{Z}_n$ quiver theory given by the graph dual of the dimer lattice shown in figure (4).

B with common edge e, we have:

$$h_{PM}(A) - h_{PM}(B) = \left\{ \begin{array}{l} \pm 1 \text{ if } e \notin PM \\ \mp 2 \text{ if } e \in PM \end{array} \right\} \tag{2}$$

where the overall sign is fixed by the orientation of e. The function h_{PM} determines the profile of a stepped surface.

Three dimensional crystal melting is specified by perfect matchings of the infinite honeycomb lattice. The perfect matching for the frozen crystal with no atoms removed is shown in figure (2). To visualize the crystal, it is helpful to draw a rhombus around each edge contained in the perfect matching. The corresponding stepped surface constructed from these rhombi realizes the profile of the melted crystal. See figure (3) for an example.

In an unrelated development, it has been shown that dimers on a T^2 determine the low energy dynamics of type IIB space-time filling D3-branes probing a toric Calabi-Yau singularity [11, 12, 13]. The physical origin of this T^2 was recently interpreted using mirror symmetry in [14]. In a gauge theory dimer, the faces determine gauge groups, the oriented edges shared by faces give the bifundamental matter, and the vertices give all tree level superpotential terms. Note that by infinitely extending any finite dimer model on T^2, we obtain a dimer model which tiles the plane. Indeed, the

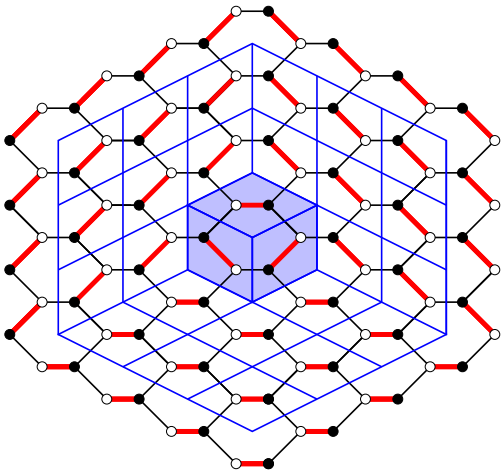

Figure 3: By surrounding each edge belonging to a perfect matching (red) by a rhombus (blue), we obtain the profile for the corresponding crystal melting configuration. The figure shows the single box crystal melting configuration (shaded).

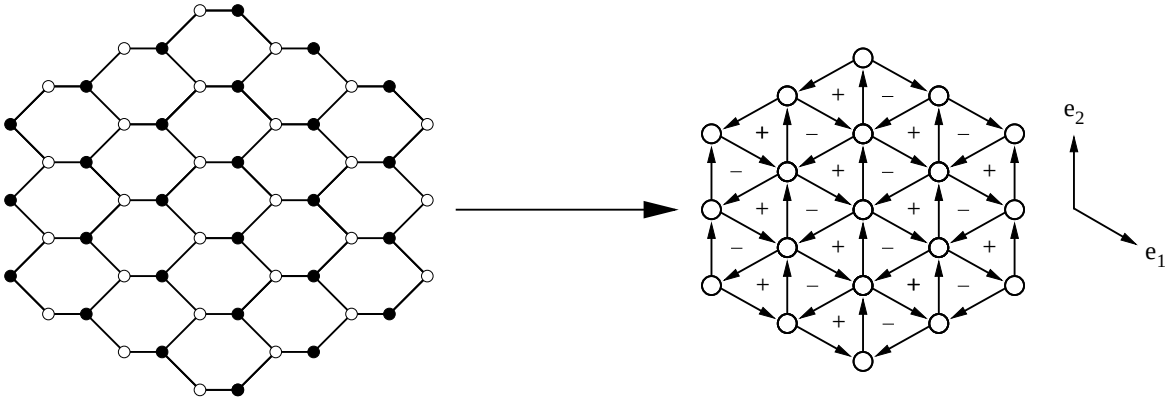

Figure 4: The graph dual of the infinite honeycomb lattice defines a quiver gauge theory. The quiver nodes determine a lattice in the complex plane with generators $e_1 = e^{-i\pi/6}$ and $e_2 = e^{i\pi/2}$. Superpotential terms are given by signed chiral gauge invariant operators constructed from triangles enclosing a single + or − .

original motivation for this note was to give a physical interpretation of the infinite honeycomb lattice dimer model of crystal melting purely as a quiver gauge theory of the type shown in figure (4).

The plan of this note is as follows. In section 2 we study flops of black hole charge configurations in the local geometry $\mathbb{C}^2/\mathbb{Z}_n$ which realize 2d crystal melting configurations. We next show in section 3 that at the level of homology in the type IIB mirror of $\mathbb{C}^3/\mathbb{Z}_n \times \mathbb{Z}_n$, there are naively far too many candidate charge configurations to match to 3d crystal melting. Using technology from gauge theory dimer models, in section 4 we present a refined analysis in the bounded derived category of coherent sheaves which recovers the expected correspondence. Following this, in section 5 we connect the partition functions for crystal melting to the representation theory of algebras naturally associated to the duality groups of the orbifold theories and give a physical interpretation of this counting. Finally, in section 6 we explain the direct mathematical connection between our ensemble of black hole crystal melting configurations and topological string theory. We then conclude and discuss possible extensions of this work.

2 2d Crystals and Black Holes

Near the orbifold point, the gauged quiver quantum mechanics of branes wrapping cycles in $\mathbb{C}^2/\mathbb{Z}_\infty \times \mathbb{C}$ is given by an infinite one dimensional lattice of $U(N_i)$ quiver nodes attached by chiral superfields $X_{i,i+1}$, $Y_{i+1,i}$ and Z_i transforming in the representations $(N_i, \overline{N}_{i+1})$, $(N_{i+1}, \overline{N}_i)$ and $(N_i, \overline{N}_i)$, respectively. D-brane probes of the finite n orbifold $\mathbb{C}^2/\mathbb{Z}_n$ were first studied in [15]. The superpotential of the theory is:

$$W = \sum_{i \in \mathbb{Z}} Tr\left(Z_i X_{i,i+1} Y_{i+1,i} - Z_{i+1} Y_{i+1,i} X_{i,i+1}\right). \tag{3}$$

This is known as the A_∞^∞ quiver [16]. The "fractional branes" of the orbifold CFT correspond to wrapping D2-branes over the blown up 2-cycles given by the simple roots $\{\alpha_i\}_{i \in \mathbb{Z}}$ of the associated A-series Lie algebra. The intersection product of these cycles is up to a minus sign given by the Cartan matrix of the algebra. The charge vector:

$$Q = \sum_i N_i \alpha_i \tag{4}$$

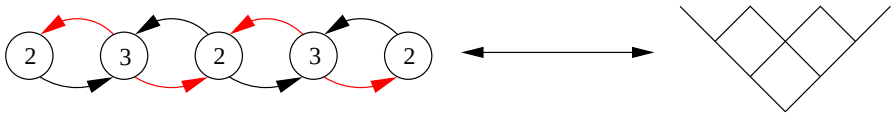

Figure 5: In 2d tableau quivers, the vertical height of the 2d tableau determines the ranks of the gauge groups. In the figure, the ranks decrease in the direction of the red arrows.

defines a quiver with gauge group $U(N_i)$ at the i^{th} node. We define a 2d tableau quiver as one where the ranks correspond to the heights of a 2d crystal.

The flop of the $\mathbb{P}^1$ corresponding to α_k is given by the Weyl reflection:

$$\sigma_{\alpha_k}(Q) = Q - (\alpha_k \cdot Q)\alpha_k \tag{5}$$

which in four dimensional gauge theories describes a Seiberg-like duality of the k^{th} quiver node [1]. From the perspective of the quiver theory, this flop corresponds to the gauge coupling g_k^{-2} becoming negative. The ranks in the flopped theory are determined by conservation of flux, or equivalently by the brane creation mechanism:

$$N_i' = N_i + (N_{k+1} + N_{k-1} - 2N_k)\,\delta_{i,k}. \tag{6}$$

The duality group of the quiver theory is generated by products of the σ_{α_i} and is isomorphic to the Weyl group of the infinite A-series algebra.

Our goal is to show that the flops of the empty room brane configuration:

$$Q_{empty} = \sum_i |i|\,\alpha_i \tag{7}$$

correspond to 2d crystal melting configurations. Weyl reflection by σ_{α_k} yields:

$$\sigma_{\alpha_k}\left(Q_{empty}\right) = Q_{empty} + 2\delta_{k,0}\alpha_0. \tag{8}$$

But this is precisely the rule for adding a box to the crystal melting configuration. Indeed, the process of adding a box to the tableau changes the height of the 0^{th} quiver node from 0 to 2. Note that the particular choice of ranks made in the empty room configuration effectively constrains the location of the non-trivial flops.

We now show that this correspondence between crystal melting and flops of 2d tableau quivers holds more generally. Given a quiver node with rank M, there are four possible rank assignments consistent with equation (1):

$$(M-1, M, M+1), (M+1, M, M-1), (M+1, M, M+1), (M-1, M, M-1). \quad (9)$$

It follows from equation (6) that in all cases a 2d tableau quiver always flops to another 2d tableau quiver. Furthermore, given two 2d tableau quivers T and $T' = T + 2\alpha_k$:

$$\sigma_{\alpha_k}(T) = T + 2\alpha_k = T'. \quad (10)$$

This implies that by acting with the duality group on the empty room configuration we can reach any 2d tableau quiver. A similar set of statements holds for the inverted empty room quiver:

$$Q_{inv} = \sum_i (N - |i|)\,\alpha_i \quad (11)$$

where $N \to \infty$ faster than $n \to \infty$ in $\mathbb{C}^2/\mathbb{Z}_n$.

Finally, in the case where n is large but finite, the quiver is given by a periodic one dimensional lattice. The empty room black hole charge configuration now has two corners about which crystal melting takes place. At finite n, the corresponding 2d tableaux begin to mix after sufficiently many flops. In [17] a similar mixing of 2d tableaux was interpreted as the non-perturbative creation of baby universes with Bertotti-Robinson cosmology $AdS_2 \times S^2$.

2.1 Duality Cascades

This same quiver also defines an $\mathcal{N} = 2$ four dimensional gauge theory described by type IIB D5-branes wrapped over the collapsed 2-cycles of the geometry. The flop transitions considered above correspond to Seiberg-like dualities of the quiver gauge theory. The 1-loop exact i^{th} holomorphic gauge coupling at scale μ is:

$$\frac{1}{g_i^2(\mu)} = \frac{(2N_i - N_{i+1} - N_{i-1})}{8\pi^2} \log\left(\frac{\mu}{\Lambda_i}\right). \quad (12)$$

This implies that local maxima in the ranks of the quiver gauge theory are asymptotically free.

Adding mass terms of the form TrZ_i^2 for all i to the superpotential of equation (3)

breaks the system to an $\mathcal{N}=1$ gauge theory of the type studied in [1]. Starting from the Q_{inv} rank assignments of equation (11), the theory will flow into the infrared, at which point it becomes appropriate to Seiberg dualize the corresponding gauge group. In this way, crystal melting corresponds to a duality cascade in renormalization group flow. Although we omit the details, it is also possible to show that by a suitable choice of couplings in the initial configuration, any sequence of adding boxes to an inverted 2d tableau can be achieved. In contrast to the original case of duality cascades on the conifold considered in [18], the cascade of this system can continue indefinitely before it confines.

3 3d Crystals and Black Holes

We now consider black hole charges parametrized by three dimensional crystal melting configurations. Interpreting the infinite honeycomb lattice as a gauge theory dimer model of the type described in the introduction, the procedure of [15] shows that the associated gauged quiver quantum mechanics system probes the supersymmetric orbifold $\mathbb{C}^3/\mathbb{Z}_n \times \mathbb{Z}_n$ in the limit of large n. The quiver nodes determine a lattice in the complex plane with generators $e_1 = e^{-i\pi/6}$ and $e_2 = e^{i\pi/2}$ and correspond to a basis of branes wrapping collapsed 2- and 4-cycles. For faces $F = ae_1 + be_2$ with $a, b \in \mathbb{Z}$, the matter content is given by bifundamentals $X_{F,F+e_1}$, $Y_{F,F+e_2}$ and $Z_{F,F-e_1-e_2}$ in the obvious notation. The superpotential is:

$$W = \sum_F Tr\left(X_{F,F+e_1} Y_{F+e_1,F+e_1+e_2} Z_{F+e_1+e_2,F} - X_{F,F+e_1} Z_{F+e_1,F-e_2} Y_{F-e_2,F}\right). \quad (13)$$

We define a 3d tableau quiver as one where the rank assignments are given by the height function of the dimer model. See figure (4) for a picture of this quiver theory.

For $\mathbb{C}^3/\mathbb{Z}_n \times \mathbb{Z}_n$, almost all of the flops of the geometry will alter the topology of the quiver and thus the classical geometry probed by the branes. In this sense, the duality group of the 2d tableau quivers is quite special because each flop preserves the intersection product of the cycles in the geometry. Even with this restriction, a preliminary analysis reveals far too many duals of the empty room quiver in comparison with crystal melting.

Because the analysis to follow is somewhat lengthy, we now give an outline of each component of sections 3 and 4. In subsection 3.1 we present a naive analysis of

geometric transitions which preserve the Calabi-Yau geometry and find far too many black hole charge configurations in comparison with crystal melting configurations. In section 4 we rectify this by determining the physical meaning of the internal perfect matchings in a general gauge theory dimer model. As explained in subsection 4.1, a candidate collection of fractional branes may contain ghost fields which render the theory unphysical. In subsection 4.2 we show that the perfect matchings of the dimer model parametrize the physical quiver theories. In appendix B we compute the effect of switching from one perfect matching to another and find that it corresponds to a subset of the transformations considered in subsection 3.1. Returning to the problem of crystal melting, we show in subsection 4.3 that the BPS black holes generated by these transformations are in one to one correspondence with crystal melting configurations. To complete our analysis, in subsection 4.4 we discuss the physical meaning of the extra charge configurations obtained in subsection 3.1.

3.1 Homology Cycles in the Mirror

To realize the flop transitions geometrically we pass to the type IIB theory on the mirror manifold $\widetilde{X}$ where worldsheet instanton corrections have been resummed into the geometry. The D0-, D2- and D4-branes which base the quiver theory in $\mathbb{C}^3/\mathbb{Z}_n \times \mathbb{Z}_n$ map to D3-branes wrapping homology 3-spheres $\Delta_i \in H_3(\widetilde{X}, \mathbb{Z})$ for $i = 1, ..., n^2$. The anti-symmetric intersection pairing $\Delta_i \cap \Delta_j$ determines the number of bifundamentals shared by Δ_i and Δ_j. The charge vector:

$$Q = \sum_i N_i \Delta_i \tag{14}$$

defines a quiver with gauge group $U(N_i)$ at the i^{th} node. In the context of Seiberg dualities of four dimensional gauge theories, flops in the mirror theory were studied in [1, 19]. We flop the brane wrapping Δ_1 by passing it through all incoming branes ($\Delta_1 \cap \Delta_{in} < 0$) for S_L duality and all outgoing branes ($\Delta_1 \cap \Delta_{out} > 0$) for S_R duality.

In the case of the infinite honeycomb lattice, we label the outgoing branes as $\Delta_2, \Delta_3, \Delta_4$ and the incoming branes as $\Delta_5, \Delta_6, \Delta_7$. Applying the transformation S_R

yields:

$$S_R\left(\Delta_1\right) = -\Delta_1 \tag{15}$$
$$S_R\left(\Delta_{out}\right) = \Delta_{out} + \left(\Delta_1 \cap \Delta_{out}\right)\Delta_1 = \Delta_{out} + \Delta_1 \tag{16}$$

where all the other Δ_i which base the quiver remain unchanged. This new basis of branes does not preserve the intersection product of the geometry. We perform a further S_R transformation by passing the brane wrapping $-\Delta_1$ through $\Delta_5, \Delta_6, \Delta_7$ to find:

$$S_R^2\left(\Delta_1\right) = -\left(-\Delta_1\right) = \Delta_1 \tag{17}$$
$$S_R^2\left(\Delta_{out}\right) = \Delta_{out} + \Delta_1 \tag{18}$$
$$S_R^2\left(\Delta_{in}\right) = \Delta_{in} + \left(-\Delta_1 \cap \Delta_{in}\right)\left(-\Delta_1\right) = \Delta_{in} - \Delta_1 \tag{19}$$

or,

$$S_R^2\left(\Delta_j\right) = \Delta_j + \left(\Delta_1 \cap \Delta_j\right)\Delta_1 \tag{20}$$

for all j. The intersection product is now unchanged:

$$S_R^2\left(\Delta_i\right) \cap S_R^2\left(\Delta_j\right) = \Delta_i \cap \Delta_j. \tag{21}$$

Conservation of flux determines the ranks of the gauge groups:

$$\sum_{i=1}^{7} N_i\Delta_i = S_R^2\left(N_1\right)\Delta_1 + \sum_{i=2}^{4} S_R^2\left(N_i\right)\left(\Delta_i + \Delta_1\right) + \sum_{i=5}^{7} S_R^2\left(N_i\right)\left(\Delta_i - \Delta_1\right) \tag{22}$$

so that:

$$S_R^2\left(N_i\right) = N_i + \delta_{i,1}\left(\sum N_{in} - \sum N_{out}\right) \tag{23}$$

in the obvious notation. A similar analysis yields:

$$S_L^2\left(N_i\right) = N_i + \delta_{i,1}\left(\sum N_{out} - \sum N_{in}\right). \tag{24}$$

Now apply the S_R^2 transformation to any node of the empty room quiver with rank assignments as in figure (2). First consider any face in the dimer model with two edges in the perfect matching. In this case, inspection of figure (2) implies that $S_R^2(N_1) = N_1$. For the face with three edges in the perfect matching, $N_1 = 0$,

$N_{2,3,4} = 1$ and $N_{5,6,7} = 2$ so that:

$$S_R^2(N_1) = 0 + (2 + 2 + 2 - 1 - 1 - 1) = +3. \tag{25}$$

This matches the change in the height function from crystal melting. Note that the transformation S_L^2 would have produced a negative rank gauge group.

To show that any crystal melting black hole charge configuration may be reached by a sequence of S_R^2 transformations, dualize the face of a 3d tableau quiver where all incoming edges belong to the perfect matching. The rank assignments are:

$$N_{F+e_i} = N_{F-e_1-e_2} = N_F + 1 \text{ (outgoing)} \tag{26}$$

$$N_{F-e_i} = N_{F+e_1+e_2} = N_F + 2 \text{ (incoming)} \tag{27}$$

for $i = 1, 2$. Applying the transformation S_R^2 yields:

$$S_R^2(N_F) = N_F + \left(\sum N_{in} - \sum N_{out}\right) = N_F + 3. \tag{28}$$

This matches the change in height of the crystal. By induction, we can reach any 3d tableau quiver by successive S_R^2 transformations of the empty room quiver.

But at the level of homology, this is not the full collection of rank assignments which S_R^2 generates. Applying the transformation S_R^2 n times yields:

$$\left(S_R^2\right)^n (N_F) = N_F + 3n \tag{29}$$

which is a much larger spectrum of BPS black holes. As we show in section 4, *none* of these extraneous charge configurations are stable.

4 Fractional Branes and Dimers

To obtain a more refined physical description of admissible S_R^2 transformed brane configurations, we pass to the bounded derived category of coherent sheaves on $X = \mathbb{C}^3/\mathbb{Z}_n \times \mathbb{Z}_n$, denoted $D^b(X)$. Under certain plausible assumptions, most of the results of the following subsections hold for general toric Calabi-Yau threefolds. Although a candidate collection of fractional branes in $D^b(X)$ may generate the correct quiver structure, the corresponding gauge theory must not contain any

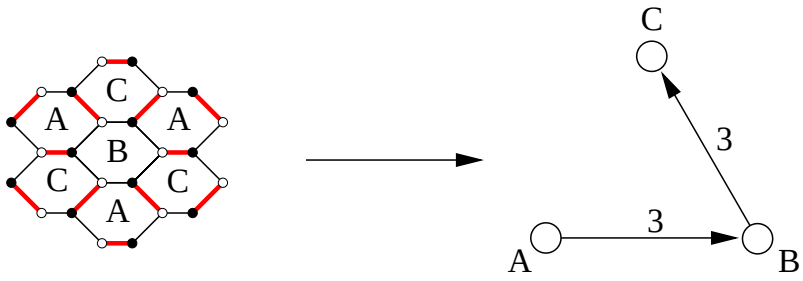

Figure 6: The gauge theory dimer model for the supersymmetric orbifold $\mathbb{C}^3/\mathbb{Z}_3$ is shown on the left. By deleting the edges belonging to the internal perfect matching (red) we obtain a Beilinson quiver which by definition contains no directed loops.

ghosts. Indeed, in subsection 3.1 we merely counted the number of bifundamentals given by the intersection product of homology cycles in the mirror and did not address the physical properties of these massless degrees of freedom. Our goal in this section is to eliminate all unphysical candidate collections.

A physical basis of fractional branes is determined by a collection of exceptional sheaves supported on a complex surface V obtained from a partial resolution of X. An exceptional collection may be thought of as a basis of branes wrapping V with the property that the associated quiver theory is obtained from the physical quiver by deleting a minimal number of bifundamentals so that no directed loops remain. An exceptional collection is called strong when the basis of fractional branes it generates contains no ghost matter. In this case, the quiver with deleted arrows is called a Beilinson quiver. See figure (6) for an example. Note that a Beilinson quiver has a certain number of starting (terminal) quiver nodes such that all attached bifundamentals are outgoing (incoming). We review in appendix A the precise definition of strong exceptional collections and their relation to fractional branes.

Although implementing these extra physical conditions appears unwieldy, it has recently been shown that in the case of gauge theory dimer models, the perfect matchings of the dimer model parametrize these exceptional collections [20]. As we show in appendix B, the local rearrangement of a perfect matching corresponds to the action of S^2_R or S^2_L on the fractional branes. This allows us to recover the expected match to crystal melting. Based on the general analysis presented in sections 4.1 and 4.2, it follows that the additional $S^2_{R,L}$ transformations of section 3.1 introduce

ghost matter into the quiver. We conjecture that the corresponding bound state decays before these ghosts are produced and explain how this picture is consistent with expectations from supergravity.

4.1 Physical Fractional Branes and Ghosts

The "fractional branes" of a physical quiver theory correspond to branes wrapping collapsed cycles in the geometry. The matter content of the quiver theory is determined by massless open strings with the appropriate Chan-Paton factors. More formally, open strings in the quiver are described by maps of the form $\mathrm{Hom}^k_{D^b(X)}(E,F)$ for $k=0,1,2,3$ with E and F in $D^b(X)$ [21]. At the orbifold point of the theory, the mass squared of the corresponding zero modes is $M_k^2=(k-1)/2$ in string units. Although the GSO projection removes the $k=0$ (and $k=2$) zero modes from the string spectrum, there are still potential instabilities in the brane system. A general collection of candidate fractional branes in $D^b(X)$ may also contain more exotic massless degrees of freedom given by bifundamental vector bosons corresponding to the first excited state of the map $\mathrm{Hom}^0_{D^b(X)}(E,F)$. These fields were interpreted in [22] as tachyons in a topological brane anti-brane system. In the physical string theory, such fields signal the presence of uncanceled ghosts [23, 24].

Whereas gauge invariance and the Ward identities ensure that all negative norm states of an adjoint valued vector boson decouple from the physical Hilbert space, no such decoupling occurs when the vector boson is in the bifundamental of two gauge groups. Indeed, the ghost number of the corresponding vertex operators in the open topological B-model shows that such fields and thus the associated quiver theories are unphysical [23]. In the case of gauged quiver quantum mechanics, these exotic bosonic propagating degrees of freedom correspond to bifundamental[2] scalars with a wrong sign kinetic term.

The kinetic term of either a physical or unphysical bifundamental scalar X is:

$$L_{kin}=c(\psi)\,Tr\left((D_0X)(D_0X)^\dagger\right) \tag{30}$$

where the real function $c(\psi)$ is a moduli dependent factor which is positive for physical matter and negative for ghost matter. The monodromy transformations

[2]For these more exotic bifundamentals, the orientation of the arrow in the quiver theory is aligned in the opposite direction to that of the associated Hom^0 map [23].

$S^2_{R,L}$ will therefore alter $c(\psi)$ and may even cause it to switch sign. Before this occurs, the system enters a regime of strong coupling where $c(\psi)$ is nearly zero. Although we do not understand the dynamics at small $c(\psi)$, we conjecture that the corresponding bound state decays before the unphysical ghost is produced. We will return to this issue in subsection 4.4.

4.2 Perfect Matchings and Exceptional Collections

To construct a basis of fractional branes which excludes the presence of ghost matter, it suffices to consider strong exceptional collections of sheaves supported on a complex surface V which may be used to generate a physical basis of fractional branes, as in [1, 8]. We now explain the connection between perfect matchings and exceptional collections.

To partially classify the perfect matchings of the dimer model, fix a reference perfect matching PM_0 and consider the formal difference of edges given by $PM - PM_0$ where PM is any other perfect matching. This formal difference determines a homology 1-cycle in the T^2 of the dimer model. As shown in [10], the corresponding subset of lattice points in $H_1(T^2, \mathbb{Z}) \simeq \mathbb{Z} \times \mathbb{Z}$ defines a convex polytope. We define an internal (external) perfect matching as one where its lattice point lies in the interior (boundary) of this polytope. The key insight of [20] was that the internal perfect matchings parametrize all possible ways of deleting a minimal number of arrows in the quiver so that no directed loops remain. Note that this is a necessary condition for forming a Beilinson quiver.

As shown in [20], up to tensoring all sheaves by a common line bundle, the internal perfect matchings of the dimer model are in one to one correspondence with exceptional collections of sheaves which generate the *same* four dimensional quiver gauge theory. On an example by example basis it was shown in [20] that each such collection is strong, so we shall assume that each exceptional collection generates a physical quiver gauge theory[3]. In other words: *The internal perfect matchings parametrize all physical collections of fractional branes which preserve both*

[3]In fact, achieving the match with crystal melting configurations does not require this stronger assumption. It follows from the discussion in section 6 that the empty room perfect matching defines a strong exceptional collection because all of the sheaves in this collection are generated by their global sections. Because all of the other internal perfect matchings of crystal melting define foundations for the same strong helix, we conclude that all of the perfect matchings of crystal melting generate physical quiver gauge theories for the large n orbifold $\mathbb{C}^3/\mathbb{Z}_n \times \mathbb{Z}_n$.

the adjacency of bifundamentals in the quiver as well as the form of the superpotential.

Now that we have a catalogue of admissible collections of fractional branes in terms of perfect matchings, we can consider the effect of switching perfect matchings. We defer this computation to appendix B where we show that changing a starting (resp. terminal) node of the associated Beilinson quiver to a terminal (resp. starting) node corresponds to a S_R^2 (resp. S_L^2) transformation.

4.3 Crystal Melting Revisited

We now specify the empty room quiver by two conditions. First, we take the ranks N_F equal to the heights h_F of the empty room perfect matching shown in figure (2). Second, we stipulate that the collection of fractional branes used to base the empty room quiver theory be derived from the same empty room perfect matching. This second condition guarantees that the corresponding Beilinson quiver has exactly one starting node at $(0,0)$ with smallest rank in the quiver gauge theory.

Because there is a single starting node in the Beilinson quiver, we may only apply the transformation S_R^2 at the node $(0,0)$. This transformation changes the node $(0,0)$ into a terminal node. Further, the three nodes $(1,0)$, $(0,1)$ and $(-1,-1)$ now correspond to starting nodes in the transformed Beilinson quiver. The change in rank of the $(0,0)$ node under S_R^2 is given by equation (28):

$$N_{(0,0)} \mapsto N_{(0,0)} + (N_{in} - N_{out}) = N_{(0,0)} + (6-3) = N_{(0,0)} + 3. \tag{31}$$

We thus see that the change in ranks exactly coincides with the change in heights from switching perfect matchings. Iterating again, there are now three candidate starting nodes for the Beilinson quiver. We may apply S_R^2 to any of these nodes to obtain another 3d tableau black hole. Combining this with the analysis done around equation (28), we conclude that: *The spectrum of BPS black hole charge configurations which are generated by geometry preserving flops of the empty room charge configuration are parametrized by 3d crystal melting configurations.*

4.4 Extra Charges, Attractors and Ghosts

At a formal level, we have parametrized the collection of fractional brane configurations which can be used to base the quiver theory. Even so, it is important to identify the explicit physical mechanism which prevents additional charges from

appearing in the single particle BPS spectrum. To this end, we review the decay of single particle objects first in the context of Seiberg-Witten theory and then in the context of the attractor mechanism for four dimensional Calabi-Yau black holes. We conjecture that before the transformation S_R^2 produces ghost matter, a similar process causes the brane configuration to decay.

First consider the four dimensional $\mathcal{N} = 2$ $SU(2)$ gauge theory studied by Seiberg and Witten in [25]. The moduli space of the theory is parametrized by the coordinate $u = \langle Tr\phi^2 \rangle$ where ϕ denotes the adjoint valued Higgs field. The electric and magnetic charge numbers (n_m, n_e) determine the central charge vector $Z = n_m a_D + n_e a$ where $a(u)$ denotes the scalar component of the $\mathcal{N} = 2$ $U(1)$ "photon" vector multiplet and $a_D(u)$ is its conjugate magnetic dual. By a suitable choice of renormalization scheme, the magnetic monopole with charge $(1, 0)$ becomes massless near the point $u = 1$. At weak coupling, applying monodromy transformations about the point $u = 1$ produces a tower of BPS charges given by $(1, n)$ and $(-1, -n)$ for integers n. At strong coupling, however, only the charge configurations $(1, 0)$ and $(1, 1)$ remain in the single particle BPS spectrum. Indeed, in the process of performing the monodromy transformation about the point $u = 1$, a given BPS state will cross a curve of marginal stability with a_D/a real. At this curve, such a state may decay into a multi-particle state of the form $S_1 + S_2$. This same conclusion was reached in the derived category by more rigorous means using notions of Π-stability in [26].

This entire discussion embeds as the low energy limit of type II string theory compactified on a rigid Calabi-Yau threefold. From the perspective of four dimensional Calabi-Yau black holes in $\mathcal{N} = 2$ supergravity, the above truncation on the spectrum is also expected. To understand this, we first recall some facts about the attractor mechanism for four dimensional BPS black holes in asymptotically flat space [27, 28, 29, 30]. Although the entropy of such black holes depends on the near horizon values of the vector multiplet moduli, these values are fixed by the charges of the black hole. The position dependence of the vector multiplet moduli is specified by an attractor flow in moduli space. As explained in [31, 32], if an attractor flow defined by a homology 3-cycle Q passes a branch cut in moduli space produced by a conifold point where a 3-cycle Δ shrinks to zero size, it will instead flow to a fixed

point with charge given by Picard Lefschetz theory:

$$Q' = Q \pm (\Delta \cap Q)\, \Delta \tag{32}$$

$$= S^2_{R,L}(Q) \tag{33}$$

where in the above we have used the mirror type IIB language. Now consider an attractor flow which circles the conifold point n times and naively produces infinitely many different charge configurations. As explained in [31], after the flow crosses the branch cut for the first time, a new wall of marginal stability appears which extends out from the conifold point. Upon crossing this wall, the attractor flow will split into two constituent products, one of which becomes massless as it flows to the conifold point. We thus obtain from a different perspective the same truncation. An analysis of monodromies and Π-stability in the derived category was presented in [33].

We conjecture that a similar set of decays occur for 3d tableau BPS black holes. Although a full analysis is beyond our reach, we can still sketch an argument of what we expect to happen. Because the action of $S^2_{R,L}$ corresponds to a monodromy transformation around a singular point in moduli space, the coefficient $c(\psi)$ of equation (30) is sensitive to this change. We suspect that this variation in the moduli causes the gauged quiver quantum mechanics to become strongly coupled before $c(\psi)$ changes sign. To prevent the appearance of ghosts, the brane system must develop a tachyonic mode and decay to some constituent products.

5 Black Hole Ensembles and Characters

As mentioned in the introduction, the untwisted RR D0-brane charge of a black hole charge configuration realized by branes wrapped on cycles in the orbifolds $\mathbb{C}^2/\mathbb{Z}_n$ and $\mathbb{C}^3/\mathbb{Z}_n \times \mathbb{Z}_n$ is given by the sum over ranks in the gauged quiver quantum mechanics:

$$Q^{(0)}_{RR}\,(BH) = \frac{1}{|\Gamma|}\sum_i N_i \equiv \frac{d}{|\Gamma|}\varepsilon\,(BH) \tag{34}$$

where $|\Gamma| = n, n^2$ and $d = 2, 3$ for $\mathbb{C}^2/\mathbb{Z}_n$ and $\mathbb{C}^3/\mathbb{Z}_n \times \mathbb{Z}_n$, respectively. Summing over all black holes which are generated by geometry preserving flops of the empty

room charge configurations yields the crystal melting partition functions:

$$Z_{BPS} = \sum_{BH} q^{\varepsilon(BH)} = Z_{crystal} = \left\{ \begin{array}{l} \prod_{n\geq 1} (1-q^n)^{-1} \quad (2\text{d}) \\ \prod_{n\geq 1} (1-q^n)^{-n} \quad (3\text{d}) \end{array} \right\}. \tag{35}$$

These partition functions are characters of the basic representations of the infinite dimensional algebra sl_∞ and the affine algebra $\widehat{sl}\,(\infty)$ at large central charge. We refer to appendices C and D for the definitions and representation theory of these algebras. Under the action of the Weyl group, the orbit of the highest weight λ of the basic representation $L\,(\lambda)$ of an infinite dimensional algebra $\mathcal{A}$ generates the weight system Ω_λ[4]. In the cases we study, the multiplicity of each weight in $L\,(\lambda)$ is unity. It therefore follows that the orbit of λ under the action of the Weyl group generates the representation. Because the Weyl groups of the algebras sl_∞ and $\widehat{sl}\,(\infty)$ coincide with the duality groups of the $\mathbb{C}^2/\mathbb{Z}_\infty$ and $\mathbb{C}^3/\mathbb{Z}_\infty \times \mathbb{Z}_\infty$ quiver theories[5], we conclude that the 2d and 3d inverted empty room black holes correspond to highest weight states of the basic representations of sl_∞ and $\widehat{sl}\,(\infty)$, respectively. We now discuss the physical origin of these algebras.

Although it is well known that the orbifold theory $\mathbb{C}^2/\mathbb{Z}_n$ produces an enhanced $SU(n)$ gauge symmetry in the uncompactified directions of the space-time, it is less clear whether a similar enhanced gauge symmetry is produced by the orbifold $\mathbb{C}^3/\mathbb{Z}_n \times \mathbb{Z}_n$. Nevertheless, the similarities between the algebras sl_∞ and $\widehat{sl}\,(\infty)$ and their analogous roles in describing crystal melting suggest that at large n the orbifold $\mathbb{C}^3/\mathbb{Z}_n \times \mathbb{Z}_n$ produces the more exotic affine gauge symmetry $\widehat{SU}(n)$ in the limit of large central charge. In this language, the sum over ranks records the diagonal $U(1)$ charge remaining after resolving the geometry.

[4]This follows from the definition of the Weyl group of an algebra. Essentially quoting from [34], the Weyl group W of an algebra $\mathcal{A}$ is the group of automorphisms of the Cartan subalgebra which are restrictions of conjugations by elements of A, the group obtained via exponentiation of $\mathcal{A}$.

[5]In the case of sl_∞, this is immediate. In the case of $\widehat{sl}\,(\infty)$, we use the fact that the specialized character of the basic representation coincides (in the limit of large central charge) with the partition function of crystal melting. Because the Weyl group of $\widehat{sl}\,(\infty)$ generates the weight system for the basic representation, we conclude that each weight appears with multiplicity one, and that correspondingly, the orbit of the highest weight under the action of the Weyl group generates the representation.

5.1 2d Crystals and sl_∞

We now show that the 2d inverted tableau charge Q_{inv} of equation (11) is the highest weight state of the basic representation of sl_∞. Some background on the representation theory of sl_∞ is collected in appendix C. Let $\{\alpha_i\}_{i\in\mathbb{Z}}$ denote the simple roots and $\{\omega_i\}_{i\in\mathbb{Z}}$ the fundamental weights of sl_∞. The relation:

$$\frac{1}{2}Q_{inv}\cdot\alpha_i=\delta_{i,0} \tag{36}$$

for all i implies the formal identification:

$$\omega_0\sim\frac{1}{2}Q_{inv}. \tag{37}$$

The specialized character of the irreducible representation $L(\omega_0)$ is [35]:

$$ch_{L(\omega_0)}(t\rho)=\sum_{\mu\in\Omega_{\omega_0}}m_\mu(\omega_0)\,e^{(\omega_0\cdot\rho-j(\mu))t}=q^{-\omega_0\cdot\rho}\prod_{n\geq1}(1-q^n)^{-1} \tag{38}$$

where $j(\mu)$ denotes the depth of the weight μ, $q=e^{-t}$, $m_\mu(\omega_0)$ $(=1)$ is the multiplicity of μ and the Weyl vector ρ is the sum over all the ω_i. We next compute the regulated dot product:

$$\rho\cdot\frac{1}{2}Q_{inv}=\frac{1}{2}\lim_{N\to\infty}\sum_{i=-N/2}^{N/2}-|i|=-\frac{1}{2}\sum_{i=1}^{\infty}i=\frac{1}{24} \tag{39}$$

which implies:

$$ch_{L_{inv}}(q)=q^{-1/24}\prod_{n\geq1}(1-q^n)^{-1}=\eta(q)^{-1} \tag{40}$$

where η is the Dedekind eta function and we have switched notation to emphasize the interpretation of Q_{inv} as a highest weight state. Finally, we note that the basic representation of sl_∞ is identical to the chiral boson representation of the Virasoro algebra. The details of the mapping between representations of sl_∞ and the Virasoro algebra may be found in [34, 35].

5.2 3d Crystals and $\widehat{sl}(\infty)$

In the type IIB mirror theory, the intersection of the 3d inverted empty room charge configuration Q_{inv} with the homology 3-cycles $\Delta_{(a,b)}$ which base the quiver theory is:

$$\frac{1}{3}Q_{inv} \cap \Delta_{(a,b)} = \delta_{(0,0),(a,b)}. \tag{41}$$

This is the 3d inverted tableau quiver analogue of equation (36).

We now show that the 3d inverted empty room charge configuration Q_{inv} defines a highest weight state for a representation of the affine algebra $\widehat{sl}(\infty)$ with central charge $C \to \infty$. To this end, we show that the character of the basic representation reproduces the 3d crystal melting partition sum. Because the orbit of the highest weight state under the Weyl group generates this representation, we conclude that the inverted empty room black hole is a highest weight state of $\widehat{sl}(\infty)$ and that the dual charge configurations are generated by the action of the Weyl/duality group of $\widehat{sl}(\infty)$. See appendix D for details on $\widehat{sl}(\infty)$ as well its relation to the $W_{1+\infty}$ algebra.

The unitary representations of this algebra are realized by tensoring $C \geq 0$ bc systems with conformal weights $\lambda_i + 1$ and $-\lambda_i$ for the i^{th} system. In the case $\lambda_i = \lambda$ for all i, the specialized character of the associated unitary irreducible representation $L(\lambda, C)$ is [36, 37]:

$$ch_{L(\lambda,C)} = Trq^{L_0} = q^{\frac{1}{2}\lambda(\lambda-1)C}\prod_{j=1}^{\infty}\prod_{k=1}^{C}\left(1-q^{j+k-1}\right)^{-1}. \tag{42}$$

Expanding this product yields:

$$ch_{L(\lambda,C)} = q^{\frac{1}{2}\lambda(\lambda-1)C}\prod_{j=1}^{\infty}\left(1-q^{j}\right)^{-1}\left(1-q^{j+1}\right)^{-1}\cdots\left(1-q^{j+C-1}\right)^{-1} \tag{43}$$

$$= q^{\frac{1}{2}\lambda(\lambda-1)C}\left(\sum_{n=0}^{C}p_{3d}(n)q^{n} + O(q^{C+1})\right) \tag{44}$$

where $p_{3d}(n)$ denotes the number of crystal melting configurations with n boxes. As $C \to \infty$ the character of $L(\lambda, C)$ tends to the partition function for 3d crystal melting. In fact, as explained in [36], the states at levels less than C coincide with

those of the quasifinite Verma module given in appendix D by equation (98).

Roughly speaking, C is an upper bound on the number of 2d tableaux given by diagonally slicing a three dimensional crystal melting configuration. This implies that in the large n orbifold $\mathbb{C}^3/\mathbb{Z}_n \times \mathbb{Z}_m$, $m \sim C$. Indeed, note that when $C = 1$ the character is:

$$ch_{L(\lambda,1)} = q^{\frac{1}{2}\lambda(\lambda-1)} \prod_{j=1}^{\infty} \left(1 - q^j\right)^{-1} \tag{45}$$

which recovers the partition function for 2d crystal melting. Finally, as observed in [38], in the limit $C \to \infty$ the basic representation of $\widehat{sl}\,(\infty)$ is closely related to the partition function of a three dimensional free field.

6 Equivariant Sheaves and Topological Strings

In this section we explain the mathematical connection between our black hole charge configurations and the crystal melting configurations of topological string theory. We also discuss the sense in which the exceptional collection defined by the empty room perfect matching is canonically determined by the geometry $\mathbb{C}^3/\mathbb{Z}_n \times \mathbb{Z}_n$. We caution that this material is more formal than other parts of this note.

The A-model partition function on $\mathbb{C}^3$ coincides with the crystal melting partition function [4]:

$$Z_A\left(\mathbb{C}^3\right) = \prod_{n \geq 1} (1 - q^n)^{-n} = Z_{\text{crystal}} \tag{46}$$

where $q = e^{-g_s}$. This is also the partition function of the six dimensional topologically twisted $U(1)$ gauge theory given by a D6-brane filling $\mathbb{C}^3$ [3]. Mathematically, the instanton configurations of the D6-brane are specified by ideal sheaves[6]. Physically, these are singular gauge field configurations which have vanishing D4-charge and D2- and D0-charge given respectively by the second and third Chern characters of the gauge bundle. The mathematical theory which counts these ideal sheaves is known as Donaldson-Thomas theory [39]. It has recently been shown that for toric Calabi-Yau threefolds, the Gromov-Witten and Donaldson-Thomas invariants coincide [40, 41]. It is believed that for more general Calabi-Yau threefolds the

[6] An ideal sheaf corresponds to a torsion free sheaf with vanishing first Chern class. For open sets U in a variety X, we define a collection of ideals $\mathcal{I}(U) \subset \mathcal{O}_X$. These local data define the corresponding ideal sheaf $\mathcal{I}$.

partition function of this six dimensional $U(1)$ gauge theory agrees with the result from Donaldson-Thomas theory.

Because $\mathbb{C}^3$ is topologically trivial, the singular gauge field configurations of the $U(1)$ gauge theory are specified by ideals I generated by monomials in the ring $\mathbb{C}[x,y,z]$. Each such ideal determines a collection of points in $\mathbb{Z}^3_{\geq 0}$:

$$\pi_I = \left\{(i,j,k) \in \mathbb{Z}^3_{\geq 0} | i,j,k \geq 1,\ x^{i-1}y^{j-1}z^{k-1} \notin I\right\}. \tag{47}$$

The D4- and D2-brane charge of such a configuration vanishes and the D0-brane charge is given by the total number of points in π_I [3].

In the rest of this section we explain how these ideals are generated from the perspective of the gauged quiver quantum mechanics. Our strategy will be to exploit the dual meaning of perfect matchings in the two systems. On the one hand, such perfect matchings parametrize crystal melting configurations, and hence ideal sheaves of $\mathbb{C}^3$. On the other hand, these same perfect matchings parametrize exceptional collections of sheaves with support on some complex surface in a resolution of the large n orbifold $\mathbb{C}^3/\mathbb{Z}_n \times \mathbb{Z}_n$. In the case of crystal melting configurations, this complex surface is defined by the canonical resolution of the orbifold singularity.

We first explain the connection between Γ-equivariant sheaves of $\mathbb{C}^3$ and tautological sheaves in orbifolds of the form $\mathbb{C}^3/\mathbb{Z}_n \times \mathbb{Z}_n \equiv \mathbb{C}^3/\Gamma \equiv X$ for arbitrary n. Following the discussion of the generalized McKay correspondence in [42], for each $\rho : \Gamma \to End(V_\rho)$ an irreducible representation of Γ, the eigensheaf F'_ρ on X is:

$$F'_\rho \equiv \mathrm{Hom}\left(V_\rho, \mathcal{O}_{\mathbb{C}^3}\right)^\Gamma. \tag{48}$$

The tautological sheaf F_ρ has support on the resolution $f : \tilde{X} \to X$:

$$F_\rho = f^* F'_\rho / torsion. \tag{49}$$

The generalized McKay Correspondence of [43] now implies that the F_ρ form a basis for the K-theory $K_0(\tilde{X})$ and lift to a basis for the Γ-equivariant K-theory $K_0^\Gamma(\mathbb{C}^3)$.

Although there are many crepant[7] resolutions of the orbifold $\mathbb{C}^3/\Gamma$ which are all related by flops, there is one distinguished choice such that the tautological sheaves of the resolution are given by a collection of line bundles which are generated by

[7] A crepant resolution of a singular Calabi-Yau X is a smooth resolution Y such that $c_1(Y) = 0$.

their global sections and such that any positive linear combination of the associated divisors is ample on the resolution. This resolution is a Γ-equivariant version of the $\mathbb{C}^3$ Hilbert scheme and is known as Γ-Hilb($\mathbb{C}^3$) in the mathematical literature [44].

As explained in [42] and references therein, the tautological sheaves of Γ-Hilb($\mathbb{C}^3$) may be viewed as a collection of monomials in the ring $\mathbb{C}[x, y, z]$. Specializing to the case of the large n orbifolds, we now give a local algorithm for converting an exceptional collection of sheaves supported on a complex surface in Γ-Hilb($\mathbb{C}^3$) into such a collection of monomials. Given two quiver nodes A and B of a Beilinson quiver connected by a bifundamental X_{AB}, the associated monomials are related by multiplication by x:

$$M_B = xM_A \tag{50}$$

with similar conventions for multiplication by y and z. Note that this removes the overall ambiguity of Γ-invariant monomials of the form xyz. The degrees of these monomials match the rank assignments of the gauged quiver quantum mechanics. The collection of monomials defined by the empty room perfect matching corresponds to the same collection of tautological sheaves of Γ-Hilb($\mathbb{C}^3$) discussed in [42]. Further, when F is the starting node of the perfect matching PM_0 with associated monomial M_F, the local dimer move which maps F to a terminal node sends M_F to the monomial:

$$M_F \to xyzM_F. \tag{51}$$

See figure (7) for the change from the empty room perfect matching to the single box perfect matching. Similar tilings by monomials have appeared in the mathematical literature on the McKay correspondence. See [42] and references therein for more details.

These monomials generate an ideal I_{PM} in $\mathbb{C}[x, y, z]$. Equation (51) implies that a local dimer rearrangement in the monomials translates to removing a point from the partition $\pi_{I_{PM}}$ defined by equation (47). Hence, (with suitable asymptotics) the exceptional collections of the infinite orbifold lift to monomial generators for ideal sheaves in $\mathbb{C}^3$.

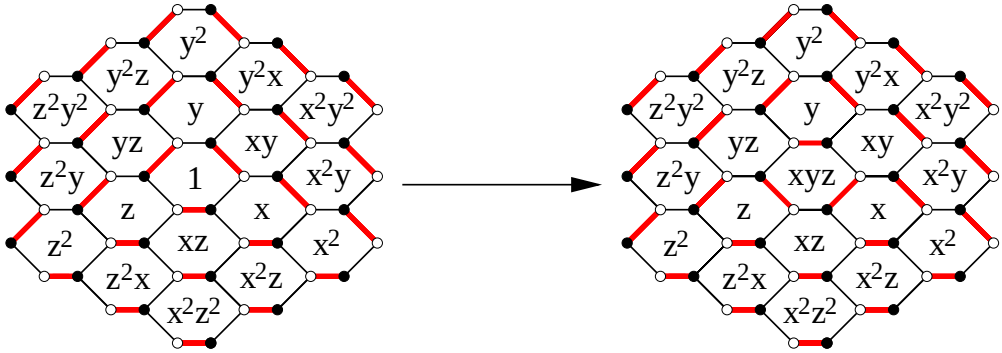

Figure 7: Each sheaf of an exceptional collection supported on the complex surface defined by the canonical resolution of $\mathbb{C}^3/\mathbb{Z}_n \times \mathbb{Z}_n$ lifts to a monomial in the variables x, y and z. The figure shows the effect of changing from the empty room perfect matching to the single box configuration. The generators of the two ideals in $\mathbb{C}[x, y, z]$ are respectively 1 and x, y, z.

6.1 2d Analogue

The partition function for two dimensional crystal melting is given by the topologically twisted $U(1)$ gauge theory of a D4-brane filling $\mathbb{C}^2$:

$$Z_{D4}\left(\mathbb{C}^2\right) = q^{-1/24} \prod_{n \geq 1} \left(1 - q^n\right)^{-1}. \tag{52}$$

Note that the extra factor of $q^{-1/24}$ agrees with the character formula of equation (40).

By resolving $\mathbb{C}^2/\mathbb{Z}_n$ we obtain a tautological sheaf for each quiver node. Each of these sheaves lifts to a monomial in $\mathbb{C}[x, y]$. The analogue of the Beilinson quiver in two dimensions is given by deleting a minimal number of arrows from the quiver so that no directed loops remain. In this case, the starting (resp. ending) nodes of the quiver have all incoming (resp. outgoing) bifundamentals deleted. When the monomials M_i and M_{i+1} are connected by the arrow $X_{i,i+1}$ (resp. $Y_{i+1,i}$), the analogue of equation (50) is $M_{i+1} = xM_i$ (resp. $M_i = yM_{i+1}$). Given a 2d Beilinson quiver with starting node i, the analogue of equation (51) is:

$$M_i \to xyM_i. \tag{53}$$

7 Conclusions

In this note we have discovered a one to one correspondence between two and three dimensional crystal melting configurations and certain type IIA BPS black holes obtained from wrapping branes on collapsed cycles of the large n orbifolds $\mathbb{C}^2/\mathbb{Z}_n$ and $\mathbb{C}^3/\mathbb{Z}_n \times \mathbb{Z}_n$. Moreover, the entire BPS spectrum of such black holes is generated by geometric transitions of brane configurations which leave the classical background geometry invariant. In the process of establishing this connection, we found a more general set of results on the physical meaning of perfect matchings in gauge theory dimer models and interpreted the associated black hole partition functions in terms of the representation theory of algebras naturally associated to the duality groups of the orbifolds. Finally, we provided a mathematical connection between these black hole crystal melting configurations and topological string theory. In the rest of this section we speculate on some possible extensions of this work.

Returning to the partition functions of section 5, consider the statistical mechanical average value of quiver ranks in the limit of uniform weighting given by $q \to 1$. By suitably rescaling the ranks and locations of quiver nodes, we obtain a limit shape for the profile of the molten crystal [45, 46, 10] which defines the charges of an average BPS black hole. In the immediate vicinity of a quiver node all of its neighboring ranks are equal. It is therefore tempting to deconstruct these quiver theories as in [47]. In our case, however, we can only deconstruct finite sized patches of the quiver. Lifting to M-theory, this suggests that after many flops a deconstructed M2-brane emerges with the gradients in the ranks signalling local changes in the worldvolume curvature.

Our analysis only treated flop transitions which leave the classical geometry probed by the branes unchanged. It would be interesting to see whether more general transitions of the orbifold theories also have an interpretation in topological string theory.

Finally, we only considered the simplest manifestation of three dimensional crystal melting given by the $\mathbb{C}^3$ Calabi-Yau crystal. As a sketch of what to expect for more general toric Calabi-Yau threefolds, we note that the mirror curve of the conifold $\mathcal{O}(-1) \oplus \mathcal{O}(-1) \to \mathbb{P}^1$ is described by dimer models on the infinite square lattice [4, 10]. Auspiciously, this is the same as the gauge theory dimer of the $\mathbb{Z}_n \times \mathbb{Z}_n$ orbifold of the conifold in the large n limit.

Acknowledgements

We thank D. Vegh for many helpful discussions and collaboration at an early stage of this work. In addition, we thank S. Franco, C. Herzog, S. Katz, L. Motl and M. Wijnholt for helpful discussions. Part of this work was performed at the 2006 Simons Workshop in Mathematics and Physics and we thank the organizers for providing a productive and stimulating environment. CV also thanks the CTP at MIT for hospitality during his sabbatical leave. The work of JJH and CV is supported in part by NSF grants PHY-0244821 and DMS-0244464. The work of JJH is also supported by an NSF Graduate Fellowship.

Appendix A: Exceptional Collections and Fractional Branes

This appendix reviews the procedure for obtaining a physical basis of fractional branes on a non-compact Calabi-Yau threefold X from an exceptional collection of sheaves supported on a possibly singular complex surface V given by partially resolving X. A good reference for additional information on exceptional collections is [48]. An exceptional collection of sheaves $\mathcal{E}^V = \left(E_1^V, ..., E_S^V\right)$ supported on V is an ordered collection of sheaves defined by the conditions:

$$\mathrm{Ext}^q\left(E_i^V, E_i^V\right) = \left\{ \begin{array}{l} 0 \text{ if } q > 0 \\ \mathbb{C} \text{ if } q = 0 \end{array} \right\} \tag{54}$$

$$\mathrm{Ext}^q\left(E_i^V, E_j^V\right) = 0 \text{ if } i > j \tag{55}$$

where $\mathrm{Ext}^{(\cdot)}$ is a generalization of cohomology for sheaves. When an exceptional collection satisfies the further property that for all $q > 0$,

$$\mathrm{Ext}^q\left(E_i^V, E_j^V\right) = 0 \text{ for all } i \neq j \tag{56}$$

it is called strong. We define a helix of sheaves $\left\{E_i^V\right\}_{i\in\mathbb{Z}}$ of period S recursively as follows:

$$E_{i+S}^V = R_{E_{i+S-1}^V}...R_{E_{i+1}^V}E_i^V \tag{57}$$

$$E_{-i}^V = L_{E_{-i+1}^V}...L_{E_{n-1-i}^V}E_{n-i}^V \quad (i \geq 0). \tag{58}$$

The notation L_E and R_E denotes respectively left and right mutations by the sheaf E. See pages 5 and 6 of [48] for the definition of mutation for sheaves. Given two sheaves (E, F) which form an exceptional pair, these mutations correspond to braiding operations which produce another exceptional pair of sheaves:

$$(E, F) \stackrel{L}{\to} (L_E F, E) \tag{59}$$

$$(E, F) \stackrel{R}{\to} (F, R_F E). \tag{60}$$

The left and right braiding operations are inverse to one another.

We refer to any exceptional collection which generates $\left\{E_i^V\right\}_{i\in\mathbb{Z}}$ as a foundation of the helix. It follows from the definitions given above that for every integer m, the collection of sheaves $(E_{m+1}^V, ..., E_{m+S}^V)$ is also a foundation of the helix $\left\{E_i^V\right\}_{i\in\mathbb{Z}}$. When a helix has a strong foundation it is called a strong helix. An important caveat is that there are multiple orderings of the sheaves inside of the helix which obey the same periodicity properties. In this sense, the indexing by the integers should be viewed as only a partial ordering[8].

As proposed in [49] and further substantiated in [21, 50, 51], a B-brane is given by a bounded complex of coherent sheaves in $D^b(X)$. Following the discussion in [6], given a strong exceptional collection of sheaves supported on V which generates the derived category of coherent sheaves on V, the corresponding basis of fractional branes in $D^b(X)$ is given by the collection of left-mutated objects lifted from $D^b(V)$ to $D^b(X)$:

$$\mathcal{E}_{Frac} = \left(L_{\delta E_1^V}...L_{\delta E_{S-1}^V}\delta E_S^V, ..., L_{\delta E_1^V}\delta E_2^V, \delta E_1^V\right) \equiv (E_S, .., , E_1) \tag{61}$$

where the notation δE denotes the complex:

$$... \to 0 \to 0 \to E \to 0 \to 0 \to ... \tag{62}$$

[8]This point was emphasized to us by C. Herzog.

with E a coherent sheaf sitting at the 0^{th} position of the complex. See page 65 of [48] for the definition of mutation for objects in the derived category. The two collections are dual in the sense that:

$$\chi\left(E_i^V, E_j\right) = \delta_{i,j} \tag{63}$$

where the pairing $\chi(A, B)$ counts with signs the massless open string modes between the branes A and B. Each strong foundation for a helix defines a physical collection of fractional branes on X which base the quiver [6, 7].

The upper triangular matrix $S_{ij} = \chi(E_j, E_i)$ with ones on the diagonal determines the adjacency of bifundamentals in the quiver gauge theory. For $i < j$, S_{ij} is the number of arrows from node j to node i minus the number from i to j. In the associated Landau-Ginzburg theory, S_{ij} corresponds to the soliton counting matrix [52]. At the level of charges, each E_i maps to a homology 3-sphere Δ_i in the mirror theory. Our sign convention is that for $i < j$:

$$S_{ij} = \chi(E_j, E_i) = \Delta_j \cap \Delta_i. \tag{64}$$

Next consider two B-branes E_i, E_j of $\mathcal{E}_{Frac}$ as in equation (61) with mirror 3-cycles Δ_i and Δ_j, respectively. For $i < j$, the Chern character of $R_{E_i}E_j$ is[9]:

$$ch\left(R_{E_i}E_j\right) = ch\left(E_j\right) - \chi\left(E_j, E_i\right) ch\left(E_i\right) = ch\left(E_j\right) - S_{ij} ch\left(E_i\right). \tag{65}$$

This maps to the mirror 3-cycle:

$$ch\left(R_{E_i}E_j\right) \to \Delta_j + \left(\Delta_i \cap \Delta_j\right)\Delta_i. \tag{66}$$

Similarly, the Chern character of $L_{E_j}E_i$ is:

$$ch\left(L_{E_j}E_i\right) = ch\left(E_i\right) - \chi\left(E_j, E_i\right) ch\left(E_j\right) = ch\left(E_i\right) - S_{ij} ch\left(E_j\right) \tag{67}$$

which maps to the mirror 3-cycle:

$$ch\left(L_{E_j}E_i\right) \to \Delta_i + \left(\Delta_i \cap \Delta_j\right)\Delta_j = \Delta_i - \left(\Delta_j \cap \Delta_i\right)\Delta_j. \tag{68}$$

[9]Note that the ordering of B-branes in equation (61) means that when $i < j$, E_i appears after E_j in the collection of fractional branes.

Comparing with the discussion in subsection 3.1, we see that an appropriate combination of right (resp. left) mutations will realize the transformation S_R^2 (resp. S_L^2) in the mirror theory.

Appendix B: Dimer Moves and Flops

In this appendix we establish the link between geometry preserving flops and local rearrangements of perfect matchings. Each internal perfect matching of a gauge theory dimer model defines an exceptional collection of sheaves supported on a complex surface obtained from a partial resolution of the toric Calabi-Yau threefold X [20]. As shown in [11], these internal perfect matchings also label the internal grid points of the toric diagram for X. When two perfect matchings correspond to the same internal grid point, they determine different foundations of the same helix. We now show that a local rearrangement of an internal perfect matching corresponds to a series of right (resp. left) mutations of the starting (resp. terminal) sheaf of the Beilinson quiver. In the mirror type IIB theory, this corresponds to the transformation S_R^2 (resp. S_L^2).

First fix an internal perfect matching PM with associated strong exceptional collection of sheaves $\mathcal{E}^{PM} = (E_1^{PM}, ..., E_S^{PM})$ supported on the complex surface V_{PM}. With conventions as in appendix A, the sheaf E_1^{PM} corresponds to a face F in the dimer model such that all of the incoming arrows of F belong to the perfect matching. Next consider the internal perfect matching PM' such that the formal difference of edges $PM - PM'$ forms a closed loop encircling the face F. This defines another exceptional collection $\mathcal{E}^{PM'} = \left(E_1^{PM'}, ..., E_S^{PM'}\right)$ with support on V_{PM}. We assume that the corresponding rearrangement of perfect matchings only alters the sheaf E_1^{PM} of the collection $\mathcal{E}^{PM}$ so that:

$$E_{i-1}^{PM'} = E_i^{PM} \tag{69}$$

for $i = 2, ..., S$. To determine the effect on the sheaf E_1^{PM}, note that the helix condition implies the collection $\left(E_2^{PM}, ..., E_S^{PM}, E_{S+1}^{PM}\right)$ is strongly exceptional. Since all of the outgoing arrows of the sheaf E_{S+1}^{PM} are absent from the associated Beilinson quiver, we conclude that[10]:

$$E_S^{PM'} = E_{S+1}^{PM} = R_{E_S^{PM}} ... R_{E_2^{PM}} E_1^{PM} \tag{70}$$

[10]We thank C. Herzog for correspondence on this point.

where the second equality follows from equation (57).

Next consider the effect of a local dimer move on a terminal node of the Beilinson quiver. In this case, an argument similar to the one given above implies that the exceptional collection of sheaves changes to:

$$E_{i+1}^{PM\prime} = E_i^{PM} \tag{71}$$

for $i = 1, ..., S-1$ and further,

$$E_1^{PM\prime} = E_0^{PM} = L_{E_1^{PM}} \cdots L_{E_{S-1}^{PM}} E_S^{PM}. \tag{72}$$

In the event that there are two possible starting (resp. terminal) nodes for the Beilinson quiver, there are then two distinct orderings of the sheaves in the exceptional collection. The two local dimer rearrangements correspond to right (resp. left) mutating the chosen starting (resp. terminal) sheaf to the right (resp. left) of all other sheaves in the collection.

We now demonstrate that the local dimer moves considered above correspond to the transformations S_R^2 and S_L^2 in the mirror theory. Given a quiver node i, we split the remaining quiver nodes into three types: those that are outgoing from i, those that are incoming to i and those that do not touch i. We label the sheaves of the exceptional collection according to this convention as well. In the case $i = 1$, we have outgoing sheaves $E_2^{PM}, ..., E_a^{PM}$ and incoming sheaves $E_{a+1}^{PM}, ..., E_S^{PM}$, where by abuse of notation we have labelled all nodes which do not touch i as incoming. Now right mutate E_1 through the outgoing sheaves. We refer to this "helix duality" as H_R. This transformation produces another exceptional collection:

$$H_R\left(\mathcal{E}^{PM}\right) = \left(E_2^{PM}, ..., E_a^{PM}, R_{E_a^{PM}} \cdots R_{E_2^{PM}} E_1^{PM}, E_{a+1}^{PM}, ..., E_S^{PM}\right). \tag{73}$$

The corresponding transformation on the basis of fractional branes was computed in [6] with the result:

$$H_R\left(\mathcal{E}_{Frac}\right) = \left(E_S, ..., E_{a+1}, \delta E_1^{PM}\left[1\right], R_{\delta E_1^{PM}} E_a, ..., R_{\delta E_1^{PM}} E_2\right) \tag{74}$$

where the the object $\mathcal{F}\left[n\right]$ in $D^b\left(X\right)$ denotes the complex $\mathcal{F}$ with all entries shifted n positions to the left. Note that the complex corresponding to the dualized node has shifted one position to the left. This has the effect of exchanging the brane for

the anti-brane and thus reverses the direction of all incoming and outgoing arrows incident on the corresponding quiver node. Performing another H_R duality therefore right mutates the sheaf $R_{E_a^{PM}} \cdots R_{E_2^{PM}} E_1^{PM}$ through the sheaves $E_{a+1}^{PM}, ..., E_S^{PM}$:

$$H_R^2\left(\mathcal{E}^{PM}\right) = \left(E_2^{PM}, ..., E_S^{PM}, R_{E_S^{PM}} \cdots R_{E_2^{PM}} E_1^{PM}\right). \tag{75}$$

The corresponding transformation on the basis of fractional branes is:

$$H_R^2\left(\mathcal{E}_{Frac}\right) = \left(\delta E_1^{PM}\left[2\right], R_{\delta E_1^{PM}[1]} E_S, ..., R_{\delta E_1^{PM}[1]} E_{a+1}, R_{\delta E_1^{PM}} E_a, ..., R_{\delta E_1^{PM}} E_2\right). \tag{76}$$

Next consider the "helix duality" H_L given by left mutating E_S^{PM} past all of its incoming sheaves. We label the incoming and outgoing sheaves as $E_{b+1}^{PM}, ..., E_{S-1}^{PM}$ and $E_1^{PM}, ..., E_b^{PM}$, respectively. Applying the transformation H_L yields:

$$H_L\left(\mathcal{E}^{PM}\right) = \left(E_1^{PM}, ..., E_b^{PM}, L_{E_{b+1}^{PM}} \cdots L_{E_{S-1}^{PM}} E_S^{PM}, E_{b+1}^{PM}, ..., E_{S-1}^{PM}\right). \tag{77}$$

The corresponding transformation on the basis of fractional branes is:

$$H_L\left(\mathcal{E}_{Frac}\right) = \left(L_{\delta E_S^{PM}} E_{S-1}, ..., L_{\delta E_S^{PM}} E_{b+1}, \delta E_S^{PM}\left[-1\right], E_b, ..., E_1\right). \tag{78}$$

As before, δE_S^{PM} has been sent to its "anti-brane", although it is now $\delta E_S^{PM}\left[-1\right]$ rather than $\delta E_S^{PM}\left[1\right]$. Performing another H_L transformation produces the exceptional collection:

$$H_L^2\left(\mathcal{E}^{PM}\right) = \left(L_{E_1^{PM}} \cdots L_{E_{S-1}^{PM}} E_S^{PM}, E_1^{PM}, ..., E_b^{PM}, E_{b+1}^{PM}, ..., E_{S-1}^{PM}\right) \tag{79}$$

with corresponding basis of fractional branes:

$$H_L^2\left(\mathcal{E}_{Frac}\right) = \left(L_{\delta E_S^{PM}} E_{S-1}, ..., L_{\delta E_S^{PM}} E_{b+1}, L_{\delta E_S^{PM}[-1]} E_b, ..., L_{\delta E_S^{PM}[-1]} E_1, \delta E_S^{PM}\left[-2\right]\right). \tag{80}$$

We recognize the transformation of equation (75) as the local rearrangement of PM given by equation (70). It follows from equation (66) that in terms of homology cycles in the mirror theory, H_R^2 corresponds to passing the brane wrapping Δ_1 through all outgoing and then all incoming branes. An analogous argument shows that the local rearrangement of PM given by equation (72) corresponds to passing the

brane wrapping Δ_S through all incoming and then all outgoing branes. Similar computations of monodromy transformations in terms of mutations have appeared in [53, 54, 55]. As discussed in [56], however, there is in general a difference between monodromy transformations and mutations in the derived category.

Finally, note that under the transformation H_R^2 (resp. H_L^2), the fractional brane corresponding to δE_1^{PM} (resp. δE_S^{PM}) shifts to $\delta E_1^{PM}[2]$ (resp. $\delta E_S^{PM}[-2]$) and also moves to a different position in the collection of fractional branes which base the quiver. We thus see that it is too naive to assume as we did in subsection 3.1 that the brane corresponding to the dualized node simply returns to itself.

Appendix C: Representations of sl_∞

This appendix reviews material from [34] and [35] on the correspondence between states in the basic representation of sl_∞ and 2d Young tableaux. These 2d tableaux also correspond to the states of the chiral boson representation of the Virasoro algebra.

The algebra sl_∞ is defined as the space of traceless infinite matrices with only finitely many non-zero entries. Given an infinite vector space V with basis $\{v_i\}_{i\in\mathbb{Z}}$, we define the infinite wedge space $F = \wedge^\infty V$ as the complex vector space spanned by "semi-infinite monomials":

$$v_{i_1} \wedge v_{i_2} \wedge ... \tag{81}$$

where $i_1 > i_2 > ...$, and $i_n = i_{n-1} - 1$ for $n >> 0$. F defines a representation r of sl_∞:

$$r(a)\,(v_{i_1} \wedge v_{i_2} \wedge ...) = (a \cdot v_{i_1}) \wedge v_{i_2} \wedge ... + v_{i_1} \wedge (a \cdot v_{i_2}) \wedge ... + ... \tag{82}$$

where $a \cdot v$ denotes matrix multiplication of the vector $v \in V$ by the matrix $a \in sl_\infty$. For each integer $m \in \mathbb{Z}$, we define a charge m vacuum vector:

$$|m\rangle \equiv v_m \wedge v_{m-1} \wedge v_{m-2} \wedge ... \tag{83}$$

and define the "charge-m" subspace $F^{(m)}$ as the linear span of all semi-infinite monomials which differ from $|m\rangle$ in only a finite number of places. F decomposes into independent charge spaces:

$$F = \underset{m\in\mathbb{Z}}{\oplus} F^{(m)}. \tag{84}$$

Each $F^{(m)}$ defines an irreducible representation of sl_∞ isomorphic to the basic representation $L(\omega_m)$, where ω_m denotes the fundamental weight such that $\omega_m \cdot \alpha_n = \delta_{m,n}$ for all simple roots α_n. The correspondence between the generators of $F^{(m)}$ and 2d partitions of the form $\{\lambda_1 \geq \lambda_2 \geq \cdots \geq 0\}$ is given by the bijection:

$$v_{i_1} \wedge v_{i_2} \wedge ... \mapsto \{\lambda_1 = i_1 - m, \lambda_2 = i_2 - (m-1), ...\}. \tag{85}$$

Because the λ_i correspond to the lengths of rows in a 2d Young tableau, we obtain the expected correspondence.

Appendix D: Representations of $\widehat{sl}(\infty)$ and $W_{1+\infty}$

This appendix reviews the representation theory of the algebras $\widehat{sl}(\infty)$ and $W_{1+\infty}$. Our discussion closely follows that in [37] where further details may be found. The algebra $\widetilde{gl}(\infty)$ consists of infinite matrices with only a finite number of non-zero diagonals. Note that this is a much larger space than gl_∞ which consists of infinite matrices with only a finite number of non-zero entries. The algebra $\widehat{gl}(\infty)$ is a central extension of $\widetilde{gl}(\infty)$ and is spanned by generators $E(r,s)$ for $r, s \in \mathbb{Z}$ subject to the commutation relations:

$$[E(r,s), E(r',s')] = \delta_{r'+s,0} E(r,s') - \delta_{r+s',0} E(r',s) + C\delta_{r+s',0}\delta_{r'+s,0}(\theta_r - \theta_{r'}) \tag{86}$$

where θ_r equals 1 for $r \geq 0$ and 0 otherwise.

The $W_{1+\infty}$ algebra is generated by polynomials of z, z^{-1} and $D \equiv z\partial_z$ subject to the commutation relations:

$$\left[W\left(z^n e^{xD}\right), W\left(z^m e^{yD}\right)\right] = (e^{mx} - e^{ny}) W(z^{n+m} e^{(x+y)D}) - C\frac{e^{mx} - e^{ny}}{e^{x+y} - 1}\delta_{n+m,0} \tag{87}$$

where $n, m \in \mathbb{Z}$, C is the central charge of the algebra and x and y are place keeping devices in the expansion of the exponentials. The Cartan subalgebra is generated by the operators $W(D^k)$ for $k \geq 0$. The generators $L_n \equiv -W(z^n D)$ span a Virasoro subalgebra with central charge $c_{VIR} = -2C$. The realization of the $W_{1+\infty}$ algebra

in terms of $\widehat{gl}(\infty)$ is given by:

$$W\left(z^n e^{xD}\right) = \sum_{\substack{r,s\in\mathbb{Z} \\ r+s=n}} e^{x(\lambda-s)} E(r,s) - C\frac{e^{\lambda x}-1}{e^x-1}\delta_{n,0} \tag{88}$$

where λ is a real parameter which we will eventually identify with the conformal weight of a field in the free field realization of the algebra. Although infinite, the above sum is restricted to the n^{th} diagonal.

A highest weight representation of $W_{1+\infty}$ is determined by a highest weight state $|\lambda\rangle$ such that:

$$W\left(z^n D^k\right)|\lambda\rangle = 0 \ (n \geq 1, k \geq 0) \tag{89}$$

$$W(D^k)|\lambda\rangle = \Delta_k |\lambda\rangle \quad (k \geq 0). \tag{90}$$

In general, the weights Δ_k may be complex numbers which we encode as coefficients in the weight function:

$$\Delta(x) = -\sum_{k\geq 0} \Delta_k \frac{x^k}{k!}. \tag{91}$$

The Verma module associated with $|\lambda\rangle$ is given by all descendants of the form:

$$W\left(z^{-n_1} D^{k_1}\right) ... W\left(z^{-n_m} D^{k_m}\right)|\lambda\rangle \tag{92}$$

where $n_i \geq 1$ and $k_i \geq 0$ for all i. From the perspective of the Virasoro subalgebra, the level of the given descendant is $n_1 + ... + n_m$. We obtain an irreducible representation of $W_{1+\infty}$ by projecting out the null states of the above module. In contrast to representations of the Virasoro algebra, note that there are an infinite number of states at each level. In spite of this, there exist representations of $W_{1+\infty}$ which have a finite number of independent states at each level [57]. Such representations are called quasifinite.

A highest weight state $|\lambda\rangle$ of $\widehat{gl}(\infty)$ is defined by the conditions:

$$E(r,s)|\lambda\rangle = 0 \qquad (r+s>0) \tag{93}$$

$$E(r,-r)|\lambda\rangle = q_r |\lambda\rangle \qquad (r \in \mathbb{Z}). \tag{94}$$

A representation of $\widehat{gl}(\infty)$ is quasifinite only when a finite number of $h_r = q_r - q_{r-1} + C\delta_{r,0}$ are different from zero [57]. The descendants of $|\lambda\rangle$ are of the form:

$$E(-r_1, -s_1) \cdots E(-r_n, -s_n) |\lambda\rangle \tag{95}$$

where $r \geq 0$ and $s \geq 1$. The commutation relation:

$$\left[W\left(D^1\right), E(r,s)\right] = (r+s) E(r,s) \tag{96}$$

implies that the state of equation (95) is an eigenstate of $W(D^1)$ with eigenvalue $-r_1 - s_1 - r_2 - s_2 - ... - r_n - s_n$. In fact, one of the key results of [57] establishes that the quasifinite representations of $\widehat{gl}(\infty)$ and $W_{1+\infty}$ are identical.

The quasifinite Verma module $V(\lambda, C)$ of the highest weight state with weight function:

$$\Delta(x) = C\frac{e^{\lambda x} - 1}{e^x - 1} \tag{97}$$

is spanned by states of the form:

$$W\left(z^{-n} D^k\right) |\mu\rangle \tag{98}$$

where $0 \leq k \leq n-1$ and $n \geq 0$ and $|\mu\rangle$ corresponds to a descendant in the module. The specialized character of the quasifinite Verma module is:

$$ch_{Verma} = Trq^{L_0} = q^{\frac{1}{2}\lambda(\lambda-1)C} \prod_{n\geq 1} (1-q^n)^{-n}. \tag{99}$$

When C is not an integer, the quasifinite Verma module is in fact an irreducible representation of $W_{1+\infty}$. Unfortunately, representations with non-integer C are not unitary, making the physical interpretation unclear. In the case of the unitary representations, the above Verma module will contain null vectors which must be projected out. Necessary and sufficient conditions for a unitary representation were found in [57] and are given by $C \in \mathbb{Z}_{\geq 0}$ and:

$$\Delta(x) = \sum_{i=1}^{C} \frac{e^{\lambda_i x} - 1}{e^x - 1} \tag{100}$$

where the λ_i are real numbers. We note that such a representation is obtained from

the tensor product of C bc systems with associated conformal weights $\lambda_i + 1$ and $-\lambda_i$ for $1 \leq i \leq C$.

References

[1] F. Cachazo, B. Fiol, K. Intriligator, S. Katz, and C. Vafa, "A Geometric Unification of Dualities," *Nucl. Phys. B* **628** (2002) 3–78, `hep-th/0110028`.

[2] D. Berenstein and M. R. Douglas, "Seiberg Duality for Quiver Gauge Theories," `hep-th/0207027`.

[3] A. Iqbal, N. Nekrasov, A. Okounkov, and C. Vafa, "Quantum Foam and Topological Strings," `hep-th/0312022`.

[4] A. Okounkov, N. Reshetikhin, and C. Vafa, "Quantum Calabi-Yau and Classical Crystals," `hep-th/0309208`.

[5] H. Ooguri, A. Strominger, and C. Vafa, "Black Hole Attractors and the Topological String," *Phys. Rev. D* **70** (2004) 106007, `hep-th/0405146`.

[6] C. P. Herzog, "Seiberg Duality is an Exceptional Mutation," *JHEP* **0408** (2004) 064, `hep-th/0405118`.

[7] P. S. Aspinwall and I. V. Melnikov, "D-branes on Vanishing del Pezzo Surfaces," *JHEP* **0412** (2004) 042, `hep-th/0405134`.

[8] M. Wijnholt, "Large Volume Perspective on Branes at Singularities," *Adv. Theor. Math. Phys.* **7** (2004) 1117–1153, `hep-th/0212021`.

[9] R. Kenyon, "An Introduction to the Dimer Model," `math.CO/0310326`.

[10] R. Kenyon, A. Okounkov, and S. Sheffield, "Dimers and Amoebae," `math-ph/0311005`.

[11] A. Hanany and K. D. Kennaway, "Dimer Models and Toric Diagrams," `hep-th/0503149`.

[12] S. Franco, A. Hanany, K. D. Kennaway, D. Vegh, and B. Wecht, "Brane Dimers and Quiver Gauge Theories," *JHEP* **0601** (2006) 096, hep-th/0504110.

[13] S. Franco, A. Hanany, D. Martelli, J. Sparks, D. Vegh, and B. Wecht, "Gauge Theories from Toric Geometry and Brane Tilings," *JHEP* **0601** (2006) 128, hep-th/0505211.

[14] B. Feng, Y.-H. He, K. D. Kennaway, and C. Vafa, "Dimer Models from Mirror Symmetry and Quivering Amoebae," hep-th/0511287.

[15] M. R. Douglas and G. Moore, "D-branes, Quivers, and ALE Instantons," hep-th/9603167.

[16] D. Benson, *Representations and Cohomology*. Cambridge University Press, 1991.

[17] R. Dijkgraaf, R. Gopakumar, H. Ooguri, and C. Vafa, "Baby Universes in String Theory," *Phys. Rev. D* **73** (2006) 066002, hep-th/0504221.

[18] I. R. Klebanov and M. J. Strassler, "Supergravity and a Confining Gauge Theory: Duality Cascades and χSB-Resolution of Naked Singularities," *JHEP* **0008** (2000) 052, hep-th/0007191.

[19] B. Feng, A. Hanany, Y.-H. He, and A. Iqbal, "Quiver Theories, Soliton Spectra and Picard-Lefschetz Transformations," *JHEP* **0302** (2003) 056, hep-th/0206152.

[20] A. Hanany, C. P. Herzog, and D. Vegh, "Brane Tilings and Exceptional Collections," *JHEP* **0607** (2006) 001, hep-th/0602041.

[21] M. R. Douglas, "D-branes, Categories and $\mathcal{N} = 1$ Supersymmetry," *J. Math. Phys.* **42** (2001) 2818–2843, hep-th/0011017.

[22] C. Vafa, "Brane/anti-Brane Systems and $U(N|M)$ Supergroup," hep-th/0101218.

[23] M. Wijnholt, "Parameter Space of Quiver Gauge Theories," hep-th/0512122.

[24] T. Okuda and T. Takayanagi, "Ghost D-branes," *JHEP* **0603** (2006) 062, hep-th/0601024.

[25] N. Seiberg and E. Witten, "Electric-Magnetic Duality, Monopole Condensation, And Confinement In $N = 2$ Supersymmetric Yang-Mills," *Nucl. Phys. B* **426** (1994) 19–52, hep-th/9407087.

[26] P. S. Aspinwall and R. L. Karp, "Solitons in Seiberg-Witten Theory and D-branes in the Derived Category," *JHEP* **0304** (2003) 049, hep-th/0211121.

[27] S. Ferrara, R. Kallosh, and A. Strominger, "$N = 2$ Extremal Black Holes," *Phys. Rev. D* **52** (1995) 5412–5416, hep-th/9508072.

[28] A. Strominger, "Macroscopic Entropy of $N = 2$ Extremal Black Holes," *Phys. Lett. B* **383** (1996) 39–43, hep-th/9602111.

[29] S. Ferrara and R. Kallosh, "Supersymmetry and Attractors," *Phys. Rev. D* **54** (1996) 1514–1524, hep-th/9602136.

[30] S. Ferrara and R. Kallosh, "Universality of Supersymmetric Attractors," *Phys. Rev. D* **54** (1996) 1525–1534, hep-th/9603090.

[31] F. Denef, "Supergravity Flows and D-brane Stability," *JHEP* **0008** (2000) 050, hep-th/0005049.

[32] F. Denef, B. R. Greene, and M. Raugas, "Split Attractor Flows and the Spectrum of BPS D-branes on the Quintic," *JHEP* **0105** (2001) 012, hep-th/0101135.

[33] P. S. Aspinwall, R. P. Horja, and R. L. Karp, "Massless D-Branes on Calabi-Yau Threefolds and Monodromy," *Comm. Math. Phys.* **259** (2005) 45–69, hep-th/0209161.

[34] V. G. Kac and A. K. Raina, *Bombay Lectures on Highest Weight Representations of Infinite Dimensional Lie Algebras.* World Scientific Publishing Co., Inc., 1987.

[35] V. G. Kac, *Infinite Dimensional Lie Algebras, third ed.* Cambridge University Press, 1990.

[36] E. Frenkel, V. Kac, A. Radul, and W.-Q. Wang, "$\mathcal{W}_{1+\infty}$ and $\mathcal{W}(gl_N)$ with Central Charge N," *Comm. Math. Phys.* **170** (1995) 337–358, `hep-th/9405121`.

[37] H. Awata, M. Fukuma, Y. Matsuo, and S. Odake, "Representation Theory of the $W_{1+\infty}$ Algebra," *Prog. Theor. Phys. Suppl.* **118** (1995) 343–374, `hep-th/9408158`.

[38] H. Awata, M. Fukuma, Y. Matsuo, and S. Odake, "Determinant Formulae of Quasi-Finite Representation of $W_{1+\infty}$ Algebra at Lower Levels," *Phys. Lett. B* **332** (1994) 336–344, `hep-th/9402001`.

[39] S. Donaldson and R. Thomas, "Gauge Theory in Higher Dimensions," in *The Geometric Universe: Science, Geometry, and the Work of Roger Penrose* (S. Huggett et. al, ed.). Oxford Univ. Press, 1998.

[40] D. Maulik, N. Nekrasov, A. Okounkov, and R. Pandharipande, "Gromov-Witten Theory and Donaldson-Thomas Theory, I," `math.AG/0312059`.

[41] D. Maulik, N. Nekrasov, A. Okounkov, and R. Pandharipande, "Gromov-Witten Theory and Donaldson-Thomas Theory, II," `math.AG/0406092`.

[42] M. Reid, "McKay Correspondence," `alg-geom/9702016`.

[43] T. Bridgeland, A. King, and M. Reid, "Mukai Implies McKay: the McKay Correspondence as an Equivalence of Derived Categories," *J. Amer. Math. Soc.* **14** (2001) 535–554, `math.AG/9908027`.

[44] I. Nakamura, "Hilbert Schemes of Abelian Group Orbits," *J. Alg. Geom.* **10** (2001) 757–779.

[45] R. Cerf and R. Kenyon, "The Low-Temperature Expansion of the Wulff Crystal in the 3D Ising Model," *Comm. Math. Phys.* **222** (2001) no. 1, 147–179.

[46] A. Okounkov and N. Reshetikhin, "Correlation Function of Schur Process with Application to Local Geometry of a Random 3-Dimensional Young Diagram," *J. Amer. Math. Soc.* **16** (2003) no. 3, 581–603.

[47] N. Arkani-Hamed, A. G. Cohen, D. B. Kaplan, A. Karch, and L. Motl, "Deconstructing (2,0) and Little String Theories," *JHEP* **0301** (2003) 083, `hep-th/0110146`.

[48] A. N. Rudakov et al., ed., *Helices and Vector Bundles: Seminaire Rudakov*, vol. 148 of *London Mathematical Society Lecture Note Series*. Cambridge University Press, 1990.

[49] M. Kontsevich, "Homological Algebra of Mirror Symmetry," in *Proceedings of the International Congress of Mathematicians*, pp. 120–139. Birkhauser, 1995;. `alg-geom/9411018`.

[50] M. R. Douglas, B. Fiol, and C. Romelsberger, "The Spectrum of BPS Branes on a Noncompact Calabi-Yau," *JHEP* **0509** (2005) 057, `hep-th/0003263`.

[51] D. E. Diaconescu and M. R. Douglas, "D-branes on Stringy Calabi-Yau Manifolds," `hep-th/0006224`.

[52] K. Hori, A. Iqbal, and C. Vafa, "D-branes and Mirror Symmetry," `hep-th/0005247`.

[53] S. Govindarajan and T. Jayaraman, "D-branes, Exceptional Sheaves and Quivers on Calabi-Yau Manifolds: From Mukai to McKay," *Nucl. Phys. B* **600** (2001) 457–486, `hep-th/0010196`.

[54] A. Tomasiello, "D-branes on Calabi-Yau Manifolds and Helices," *JHEP* **0102** (2001) 008, `hep-th/0010217`.

[55] P. Mayr, "Phases of Supersymmetric D-branes on Kahler Manifolds and the McKay Correspondence," *JHEP* **0101** (2001) 018, `hep-th/0010223`.

[56] P. S. Aspinwall, "Some Navigation Rules for D-brane Monodromy," *J. Math. Phys.* **42** (2001) 5534–5552, `hep-th/0102198`.

[57] V. Kac and A. Radul, "Quasifinite Highest Weight Modules Over the Lie Algebra of Differential Operators on the Circle," *Comm. Math. Phys.* **157** (1993) 429–457.